

Design of a compact bistable mechanism based on dielectric elastomer actuators

Maurizio Follador · Matteo Cianchetti · Barbara Mazzolai

Received: date / Accepted: date

Abstract Bistable mechanisms are widely used in the applications where two stable positions must be held for long time without energy consumption. The main advantage of bistable mechanisms is a sensible reduction in bulkiness and energy cost. Among the possible active triggering systems, dielectric elastomer actuators (DEA) are gaining attention, for their efficiency and strain rate, as a viable alternative to traditional technologies. In the present work, a novel design of a bistable system is proposed, counting on a cross-like shape bistable element coupled with two axially arranged conical DEAs. Analytical and FEM models have been used to implement and analyze the behavior of the single components and the final coupled system. The obtained results confirm the feasibility of the switching process between the equilibrium points and the capability to capture and numerically describe the interactions between the actuators and the bistable beams. A specific device has been finally envisaged to exemplify the possibility to develop a light-weight and compact system able to sustain and passively maintain a linear displacement which equals the 46% of its own total length.

Keywords bistable mechanism · dielectric elastomer actuator · soft actuators · FEM model

M. Follador and B. Mazzolai
Istituto Italiano di Tecnologia (IIT)
Center for Micro-BioRobotics
Viale Rinaldo Piaggio 34 56025, Pontedera (Pisa) - Italy
Tel.: +39-050-883406
Fax: +39-050-883101
E-mail: maurizio.follador@iit.it

M. Cianchetti
The BioRobotics Institute - Scuola Superiore Sant'Anna
Viale Rinaldo Piaggio 34 56025, Pontedera (Pisa) - Italy

1 Introduction

Bistable mechanical systems possess two distinct equilibrium positions, which do not need any external energy to be maintained [1]. From the point of view of the internal energy of the system, there are two minimum points which are separated by a local maximum. The difference between the maximum and the minimum represent the amount of energy that has to be provided to the system to switch from one equilibrium position to the other [2]. Typically, the additional energy that induces the change in the configuration of the system is provided by an external source. The mechanisms based on this principle are therefore made of a passive bistable element and one or more actuators that actively control the equilibrium state of the system by providing the necessary force to trigger the stability change [3,4]. The actuation is necessary for the switching between the minimum energy points, whereas no actuation is required in the two rest states, thus reducing the energy consumption. Another advantage is that the system is more stable and less influenced by external disturbances [5].

Bistable mechanisms can find an application as switches [1], valves [6], or binary actuators [3]. Binary actuators are the fundamental units of binary robots, which have joints that can assume only two configurations: the robot's workspace is determined by all the combinations of the positions of binary joints. In order to make a binary robot convenient compared to traditional robot, it must have a large number of joints, to increase the mobility, without adding too much weight. The ideal actuator must be simple, lightweight, inexpensive and low-powered [3]. Some examples, already present in literature, show bistable mechanisms actuated by shape memory alloys (SMAs) [7], and dielectric elas-

tomers actuators (DEAs) [8,9]. A SMA based mechanism has the advantage of maintaining compactness and lightness thanks to the high power density of the alloy, but a precise and reliable use of this technology is still subject of several ongoing studies. On the other side DEAs require high electric fields and a very precise manufacturing process, but they show higher strain rate, higher electro-mechanical coupling and small hysteresis [10]. These features make the DEAs good candidates for the proposed mechanism. DEAs have been widely studied for the application in robotics, but still a common limitation is the unsatisfactory performance in terms of lifespan, due to the electric breakdown of the dielectric film [11]. The DEAs used in the bistable mechanisms are less affected by this issue because the actuation time is limited to the switching time of the system.

In literature there are some examples of bistable mechanisms actuated by DEAs: the bistable element is typically a buckled beam [8], whereas the actuator can be shaped either as a diamond [12], a cone [3] or as a planar strip [8]. All these systems have in common an external frame which holds together the actuator and the bistable element, plus some additional mechanical supports for the actuators. This can limit the scalability of the system, and the ratio between the stroke and the total length of the device.

The aim of our work is to design a device that is simpler, more compact and lighter, maintaining the working principles and the performance of the current approaches. A simpler design results in the possibility to scale down the dimension of the system, and it helps to reduce the fabrication costs. Compared to the existing DEA bistable mechanisms, we propose a smaller system composed by fewer elements.

In section 2 the design of the bistable element and the DE actuator is described separately, with the use of analytical modelling. In the subsequent section the FEM simulations used for the modelling of the whole system are introduced and the method for the experimental tests on the cone actuator is described. In section 5 the validation of the models is discussed and the performance of the bistable device designed is shown. In the last section some concluding remarks are illustrated.

2 Design

The design that we propose is the continuation and extension of the work previously carried out by Hodgins et al. [13,14], which proposed a mechanism where the DEAs were combined with a buckled beam with a cross shape. In Hodgins et al., the buckled beam was

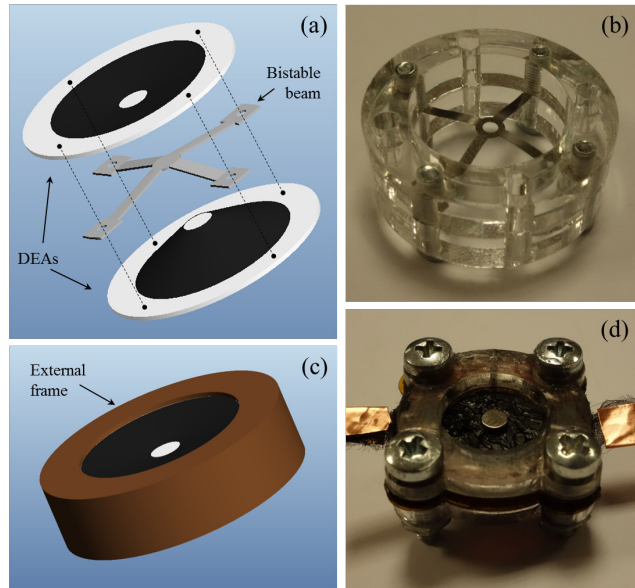


Fig. 1 a) exploded view of the CAD drawing showing the assembly of the three parts aligned (DEAs and bistable beam); b) the real bistable mechanism maintained in position by the external frame; c) CAD drawing of the entire system; d) DEA prototype with the external frame.

used as a negative rate bias spring, which could improve the actuation stroke of the conical DE actuators. The aim of the present work is to exploit the bistable property of the buckled beam to design a device with an improved linear displacement and two equilibrium positions that do not require energy to be maintained. Bistability improves the linear displacement because of the snap-through action, which can ideally double the stroke of the system presented by Hodgins et al. The design is also modified by the use of two membranes in antagonistic configuration, as shown in De Vita et al. [15], but with a more compact and simplified design.

The bistable element is the central part of the device. It is made of two buckled beams connected in the center, forming a cross shape (figure 1a and b). This element is cut from a single planar steel sheet. The cross-shaped element is constrained in the buckled configuration by a rigid frame of diameter D , by means on four screws that pass through the extremities of the beams (figure 1a). Referring to figure 2, in the frontal plane, the buckling shape is a sinusoid, with amplitude h , which is half of the total displacement of the device. The two DE membranes are arranged parallel to the xy plane.

This distance d is a design parameter, which defines the maximum displacement of the actuators. The actuators are positioned symmetrically respect to the central bistable element. Figure 1a shows the main com-

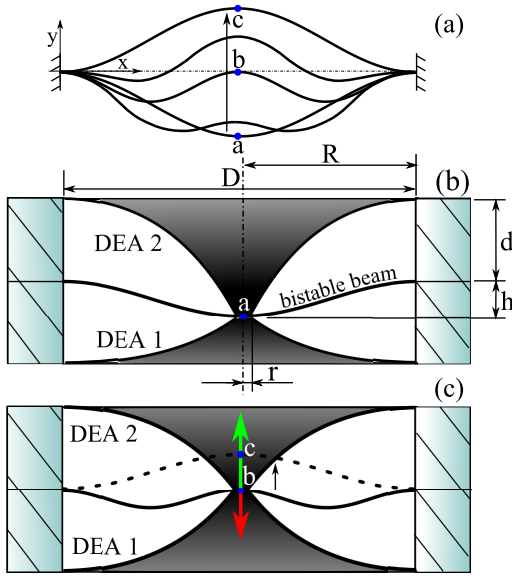


Fig. 2 a) snap-through of a constrained bistable beam, subjected to a central force, in the third mode of buckling. Point a and c are the equilibrium positions, b is the point where the snap through occurs; b) equilibrium position between the DEAs and the bistable beam, with geometrical parameters highlighted; c) snap-through due to the activation of the DEA1, represented at half of the total stroke. Arrows represents the force exerted by the active DEA1 (red), and passive DEA2 (green), with length proportional to the magnitude.

ponents of the system, with the relative positions of the various parts, whereas figure 1c and d show the real bistable beam and the DEAs respectively.

The three parts of the device are aligned and connected together in the central portion, by means of a M1 screw, through the membranes and the steel beams. In order to prevent the rupture of the membrane, it is smeared with epoxy glue in the point where the screw will pass, before applying the electrodes. The stiffness of the glue, bonded to the membrane, avoids the formation of a crack that would cause the stretched membrane to tear.

2.1 The bistable mechanism

The bistable system was modelled as two buckled beams, which are connected in the central point, to form the cross shape. The constraint in the middle prevents the asymmetric modes to occur during the transition from one equilibrium point to the other. When a vertical force is applied in the middle of the cross shape, the buckled beams deform according to the minimum energy configuration, which, in this case, is the third mode of buckling. Figure 2a shows the shapes of the bistable element during buckling. The analysis of the single beam is used to describe the mechanical characteristics of the

buckling element. The superposition principle is then used to find the actual response of the combination of the two beams. The system is linearized and decomposed in two parts. In one part, the displacement w is related to the force F applied at the centre of the beam, in the case of displacement relative to the axis of symmetry of the system ($y = \pm h$) [16]:

$$w(F) = - \left(\frac{D^3}{(n_i D)^2 EI} \right) F \left[\frac{1}{4} - \frac{1}{n_i D} \tan \left(\frac{n_i D}{4} \right) \right] \quad (1)$$

where D is the diameter of the frame that constrains the beam, E is the elastic modulus of the material, I is the moment of inertia of the beam and $n^2 = F/EI$. The subscript of n indicates the buckling mode that is considered: in the case discussed in this paper it is the third mode, and thus $n_i D = 4\pi$ (in [16] a deeper analysis of the buckling modes can be found). A coefficient that describes the spring constant for $y = 0$ can be derived substituting $n_i D = 4\pi$ in equation 1:

$$k_m = - \left(\frac{2D^3}{(4\pi)^2 EI} \right)^{-1}, \quad (2)$$

whereas the spring constant for $y = \pm h$ is [16]:

$$k_e = \frac{EI}{D^3} \left(\frac{10 - \pi^2}{16\pi^4} + \frac{EI}{(L - D) \pi^2 DEA_b - 4\pi^4 EI} \right)^{-1}, \quad (3)$$

where A_b is the cross-sectional area of the beam and L is the length of the uncompressed beam. These equations describe the force-displacement characteristic of the bistable beam, although they are linearized around the three points of zero force. The force-displacement is thus composed of three linear curves, whose intersections define the points of maximum force of the bistable beam and their coordinates. The model is used to find a first approximation of the design of the beams, which will be integrated with a FEM model to study the performance of the system during switching.

2.2 The DE actuators

The two DEAs were modelled as conical actuators, with a principle of operation similar to the one described by Berselli et al. [17]. The model was used to calculate the forces exerted by the actuators on the bistable mechanism, and thus provide the input forces for the FEM model. The actuator force is derived from the energy

functions by the application of Castigliano's theorem. The force in the vertical direction is calculated as:

$$F_y = \frac{dU_{el}}{dy} - \frac{dU_{cap}}{dy} \quad (4)$$

where U_{el} is the strain energy function of the dielectric membrane and U_{cap} is the electrical energy stored in the actuator. A second order Ogden strain energy function was used to model the hyperelastic material, using the assumption that the strain λ_c perpendicular to the radius remains constant along the radius during actuation:

$$U_{el}(\lambda_1) = \left(\frac{\mu_1}{\alpha_1} \left(\lambda_1^{\alpha_1} + (\lambda_1 \lambda_c)^{-\alpha_1} + \lambda_c^{\alpha_1} - 3 \right) + \frac{\mu_2}{\alpha_2} \left(\lambda_1^{\alpha_2} + (\lambda_1 \lambda_c)^{-\alpha_2} + \lambda_c^{\alpha_2} - 3 \right) \right) \nu \quad (5)$$

where α and μ are the Ogden parameter, λ_1 is the stretch in the radial direction, λ_c is the stretch in direction perpendicular to λ_1 and ν is the volume of the membrane. The volume is calculated as:

$$\nu = \pi (R^2 - r^2) t_0 \lambda_c^{-2} \quad (6)$$

where R is the external radius of the membrane, r the radius of the smaller face of the cone and t_0 is the thickness of the membrane in the undeformed configuration.

When there is no displacement in vertical direction, λ_1 equals λ_c , whereas the relation between the two is found with simple geometric considerations for $y > 0$:

$$\lambda_1(y) = \lambda_c \frac{\sqrt{(R-r)^2 + y^2}}{R-r} \quad (7)$$

Equation 7 is inserted in 5, in order to express the strain energy as function of y .

From the point of view of the electro-mechanical interaction, the actuator is modelled as a planar actuator, whose energy is calculated as in the case of a parallel plates capacitor:

$$U_{cap}(y, V) = \frac{\varepsilon A_e^2 V^2}{2\nu} \quad (8)$$

where ε is the dielectric constant, A_e is the area of the electrodes and V is the voltage applied between the electrodes. The area is expressed as function of the displacement y , considering it as the lateral surface of the cone, leading to:

$$A_e = \pi (R^2 + r^2) \sqrt{y^2 + (R-r)^2} \quad (9)$$

This expression is inserted in equation 8, which is then function of the displacement y and the voltage.

3 Working principle

The external force which makes the system switch its equilibrium position is provided by the DEAs. The two possible stable configurations of the system are symmetric with respect to the plane with $y = 0$ (figure 2b). In the initial state, when both DEAs are not active (point a in figure 2b), the sum of the forces is not sufficient to make the system switch configuration. After the activation of DEA1, the total force makes the bistable element move until the point where the snap-through occurs (point b in figure 2c). If the system passes that point, the bistable element snaps to another equilibrium configuration (point c in figure 2c). Figure 3 shows the scheme of the various phases of the switching, illustrated on the force-displacement curve. In the case of figure 3 the system starts in the position of negative y (P1), but it is possible also to start from the symmetric position (P3). The force of the bistable element in figure 3 was calculated with equations 2 and 3. The net forces exerted by the membranes have a direction opposite to the force of the bistable element, but they are represented with the same sign to identify the equilibrium position at the intersection of the curves. The green broken line is the net force of the DEAs when no voltage is applied. When a high DC voltage is provided to the actuator 1, the net force of the membranes changes (red dashed curve of figure 3), resulting in a net force higher than the maximum force of the bistable element. The force of the DEAs in figure 3 was derived from equation 4. The effect is a switching to position P2 (figure 3). When the voltage is removed, the system sets in position P3, because the net force of the DEAs is lower than the force of the bistable element.

The same concept can be explained in terms of internal energy of the system. The energy of the bistable system can be expressed in terms of bending energy, whereas the membrane energy can be described by the strain energy function. Figure 4 shows the energy functions for the equilibrium positions P1, P2 and P3. The total energy function of the system has initially two relative minima, symmetric to the y axis (figure 4a). In between the two minima a relative maximum acts as an energy barrier which prevents the system to change its equilibrium state without any external energy. When actuator 1 is active, the shape of the total energy varies, until the local maximum disappears and the function presents only a local minimum, which becomes the new equilibrium position (figure 4b). When the voltage is removed (figure 4c), the shape of the total energy function is the same of the figure 4a, but in this

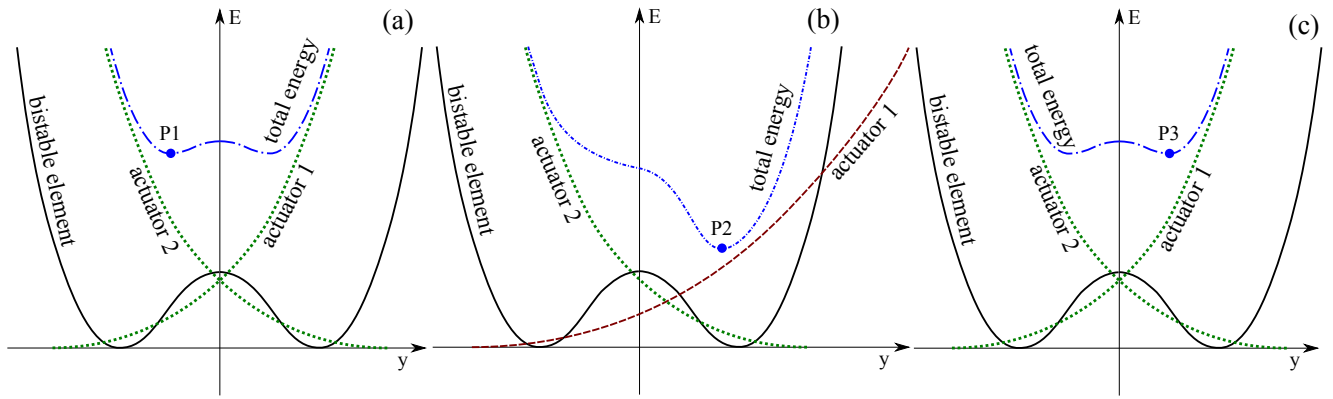


Fig. 4 Schemes of the internal energy of the system, function of the displacement y . (a) equilibrium position P1, with both actuators inactive; (b) actuator 1 is active, and the system switches to side with positive y (equilibrium point P2); (c) the actuation is removed and the system remains in position P3 (symmetric to P1) without energy consumption.

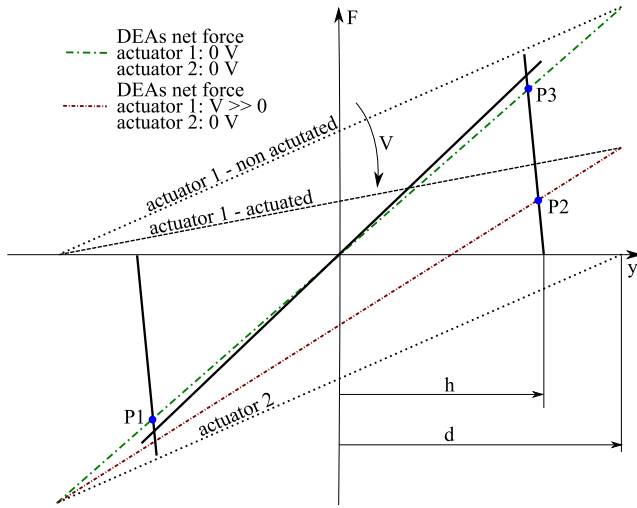


Fig. 3 Scheme of the force-displacement relation of the bistable element and the DEAs. Black dotted lines are the DE conical actuators, green broken lines is the sum of the forces of the DEAs without actuation, red dashed line is the sum of the forces of the DEAs with voltage on the actuator 1. The equilibrium positions during the switching are indicated as P1, P2 and P3. h is the maximum displacement of the bistable element, whereas d is the distance of the flat membrane.

case the energy barrier prevents the switching from P3 to P1.

4 Materials and methods

4.1 FEM model

A FEM model was developed to accurately calculate the forces exerted by the bistable element during the switching between the equilibrium states. Marc/Mentat (MSC Software) was used for the implementation of the simulation. The geometry replicated the cross-like shape of the bistable element. The mesh was imple-

mented with planar elements, imposing the boundary conditions that do not allow the system to have a deformation mode different from the prescribed one (third mode of buckling). The material (steel) was simulated as an isotropic and elastic material with Young modulus of 200 GPa. The yield stress was not included in the simulation, but the stress was calculated and then was verified that the yield limit was not exceeded.

A first simulation was implemented to validate the analytical model. It was important to quantify the difference between the analytical and the FEM model for design purpose. In particular, the maximum force exerted by the bistable element in the full range of displacement was the main characteristic needed for the design.

The overall design process can be summarized in three steps. First, the analytical models were used to find a proper combination of DEAs and bistable element, which allowed the bistability of the system. The following step was to simulate the bistable element, to verify the real mechanical properties and either confirm the accuracy of the design, or change the geometrical parameters of the bistable element or of the membranes. The final step was to simulate the combination of the DEAs and bistable elements, to evaluate the equilibrium positions. The DEAs were simulated as linear springs, connected to the center of the cross-shaped beams and constrained at a distance $y = \pm d$. The stiffness of the spring varied according to the variation of the force-displacement characteristic of the conical actuator for different actuation voltages. The resulting equilibrium position was evaluated and the bistability assessed.

4.2 Fabrication and test of the bistable element

A bistable cross-shaped element was made from a 50 μm steel shim using electrical discharge machining (EDM). The beams had a width of 1.5 mm. The four extremities of the steel element were then fixed to a circular rigid frame with an internal diameter (R) of 20 mm, causing an out of plane buckling (h) of 1.8 mm. A hole was cut at the intersection of the two beams that formed the cross, to insert a screw for the connection with the measurement setup. The setup consisted of a load cell (LSB200, Futek) rigidly connected to the centre of the bistable element, whose displacement in the y direction was controlled by a micrometric slider. The reaction force exerted by the bistable element was recorded during the motion in the full range of the stroke. The snap-through could not occur because of the constraints, thus the force-displacement curve was measured in the range $\pm h$. Results are shown in section 5.2.

4.3 Fabrication and test of the DEAs

The two DE actuators are made by a single layer of VHB 4910 (3M) with carbon grease (MG chemicals) electrodes. The acrylic film is pre-stretched uniformly and fixed on an acrylic circular frame. The grease electrodes are applied on the film after the positioning of a paper mask that delimits the area of the electrodes. Two other frames are then attached to the actuator perimeter, clamping the film and constraining the circumference. The thickness of the frame determines the distance between the plane of the rest state of the actuator and the neutral plane of the bistable mechanism. The DE conical actuator model was validated with a series of experiments on the force-displacement characteristics of DEAs. The center of the membrane was clamped between two cylindrical magnets with diameter 2 mm (N48, neodymium) and then the electrodes on each side of the VHB membrane were applied. The upper magnet was used to connect an inextensible UHMWPE cable to a micrometric linear positioning stage. The micrometric slide was equipped with a load cell (LSB200, Futek) and the motion controlled via PC. Figure 5 shows a scheme of the experimental setup for the measurements. The force and displacement were recorded on a series of experiments performed with different actuation conditions: first the test was made with no voltage between the electrodes, then an increasing voltage up to 4000 V was applied and the force-displacement curves measured. Results are shown in section 5.1.

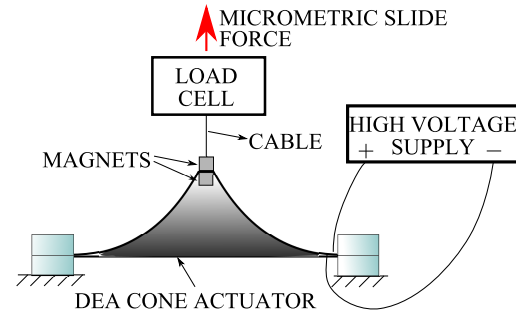


Fig. 5 Scheme of the experimental setup for the measurement of the force-displacement curve of the DEA cone actuator.

5 Results and discussion

5.1 Conical DEA validation

The results of the experimental tests for the DE actuator are shown in figure 6. The experimental results are compared to the analytical model, which was implemented using the following Ogden parameters: $\alpha_1 = 1.1$, $\mu_1 = 57$ GPa, $\alpha_2 = 5$ and $\mu_2 = 0.15$ GPa [2]. The model shows good similarity with the experiments for small displacements (from 0 to 2.5 mm), and then slightly diverges for higher displacement values. For large deformations the hypothesis made in the model regarding the preservation of a conical shape is no longer valid, and the circular pre-stretch λ_c also varies. On the other hand, the effect of the applied voltage in the model finds a good agreement with the experiments. In terms of design of the bistable mechanism, the change in the stiffness of the membrane is the most important parameter, because it determines the force difference exerted by the membranes on the beams and thus determines the bistable behavior.

5.2 Bistable beam validation

The analytical model of the bistable beam was used for the choice of the geometrical parameters for a first approximation, because it was faster and simpler than FEM models. On the other hand, the analytical model does not take into account the actual shape of the bistable element. The cross-shape adds stiffness to the structure, compared to two single buckled beams acting in parallel but not connected in the center. The FEM simulation was used to assess this effect and quantify the difference in stiffness.

The simulated geometry used the following parameters, which are the same also for the experimental tests: thickness of the beams 50 μm , width of the beams 1.5 mm, distance between the extremities of the beams in buckled configuration 20 mm, maximum displacement of

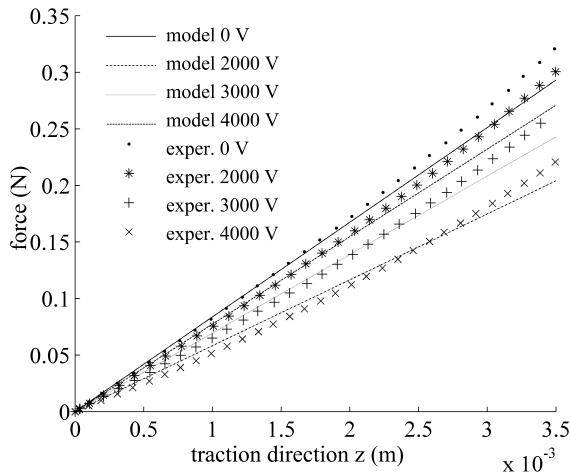


Fig. 6 Force-displacement graph of the conical DEA. Experimental tests with different actuation voltages (dotted lines) are compared to the analytic model (markers). The tested actuator had pre-stretch $\lambda_c = 3$ and diameter 20 mm.

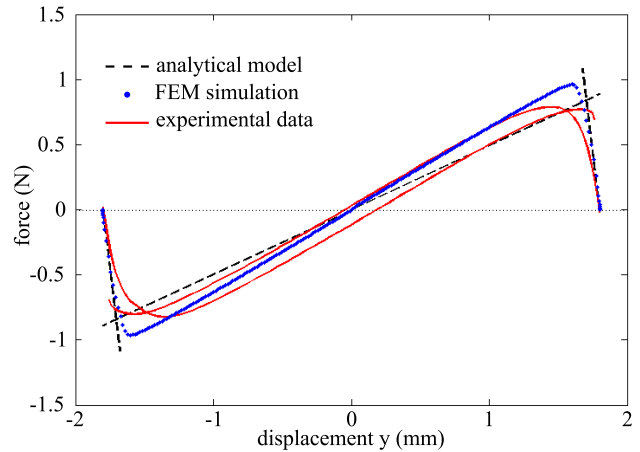


Fig. 7 Force-displacement curve of the bistable element: FEM model (blue dot marker), analytical model (black broken line) and experimental data (red line). The two experimental curves refer to the two directions of motion, indicating hysteresis during deformation.

the central point of the beams ± 1.8 mm. Figure 7 shows the comparison between the analytical, the FEM model and the experimental data. The FEM simulation confirms the linear trend of the curves subdivided in three distinct segments. A difference in the stiffness is present, as predicted, in the central part of the graph, whereas in the extremities the stiffness path is comparable. This can be explained by the different phases of actuation. Starting from one of the two stable configurations ($y = \pm h$), the force starts to increase with increasing displacement until the maximum is reached. This first segment of the curve is associated with a small displacement, and thus the effect of the stiffening due to the intersection of the beams has a small influence on the displacement-force curve. The results of the experimental tests show that the slope of the force-displacement curve can be predicted with good approximation by the FEM analysis. On the other hand, a certain hysteresis is present, which makes the point of maximum force move slightly depending on the direction of motion. Nevertheless, the maximum force is the same independently from the hysteresis, and its magnitude is comparable to the maximum force predicted by the analytical model. The information derived from the two theoretical analyses can be used to finalize the design of the bistable element in combination with the DEAs.

An optimal design of the system should maximize the force difference between the stable initial position (P1 in figure 3) and the maximum force of the bistable system. The higher is this difference, the more is the force that can be exerted by the system on the external environment. The role of the DEAs is just to provide

enough force to make the system switch to the second equilibrium position.

The design carried out with the analytic simulation was tested with a FEM simulation. The design given by the analytical models had the following parameters for the bistable beam: $h = 2.5$ mm, $d = 5$ mm, $l = 20$ mm, $t = 50$ μ m, $w = 1.5$ mm. The DEA associated with the bistable beam had a pre-stretch $\lambda_c = 4$, a diameter of 20 mm and two actuation layers. Two actuation layers can be obtained stacking two single layers made with the same fabrication process described in section 4.3. The spring rate of the conical actuator given by the analytical model was used to model the spring elements in the FEM simulations. The spring element is a mono-dimensional element with a linear spring rate. One extremity of the springs was linked to the center of the bistable element, whereas the other extremity was constrained at a distance $y = d$ and $y = -d$ respectively. A first simulation was made to define the first equilibrium position (P1), which corresponds to the case of both conical actuators not activated. Another simulation was made to calculate the second equilibrium position (P2), and thus to confirm the possibility to switch to another stability position by the DEA activation. The spring rate was varied until the switching was observed. The spring rate corresponding to an actuation voltage of 4000 V was the one that made the system switch the equilibrium position. Figure 8 shows the transition phases from position P1 to position P3. Figure 8b shows the position of maximum deformation, corresponding to the $y = 0$ coordinate of central point of the beams. The stress induced

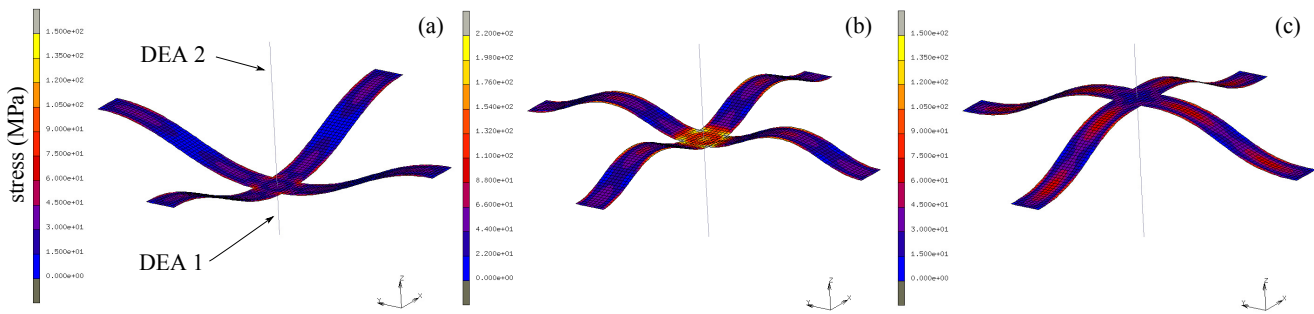


Fig. 8 Screenshots of the FEM simulation of the bistable element and the mono-dimensional springs that simulate the DEAs. (a) bistable element in position P1. The springs have the same spring rate; (b) the spring rate of spring 1 is diminished and the bistable element is switching towards position P2; (c) the system has switched in position P2 and the springs have again the same spring rate. Colorbar indicates the stress of the beams.

by bending can be calculated by the simulation: the intersection of the beams is the area where the maximum stress is observed. During the transition from P1 to P3 the stress never exceeded the yield stress of the steel (600 MPa). The graph in figure 9 shows the actual curve of force-displacement of the simulation. The black points indicate the calculated equilibrium position. In the non-actuated condition, an external force of 0.4 N is necessary to make the system switch to the opposite configuration. This force can be considered also the maximum available force that the system can exert on the environment without having a switch of the stable configuration. The total displacement of the central point of the bistable system is 4.6 mm, which corresponds to the 46% of the overall dimension of the system in the y direction (10 mm).

6 Conclusions

The design of a bistable system driven by dielectric elastomer actuators was discussed, analyzing its modelling and simulating its functioning with FEM analysis. The hypothesis of the design of a bistable mechanism with a cross-like shape was confirmed, and the FEM simulation was proved to be effective for a design more precise than the one made with the analytical models. The DEA conical actuator model and the bistable mechanism were validated with experimental analysis, and the results obtained were used to simulate the whole mechanism with a simulation that took into account the interaction of the actuators and the bistable beams. A final design of the system was provided and the forces and equilibrium positions calculated. The resulting device is light-weight, small and with a linear displacement that equals the 46% of the total length of the device.

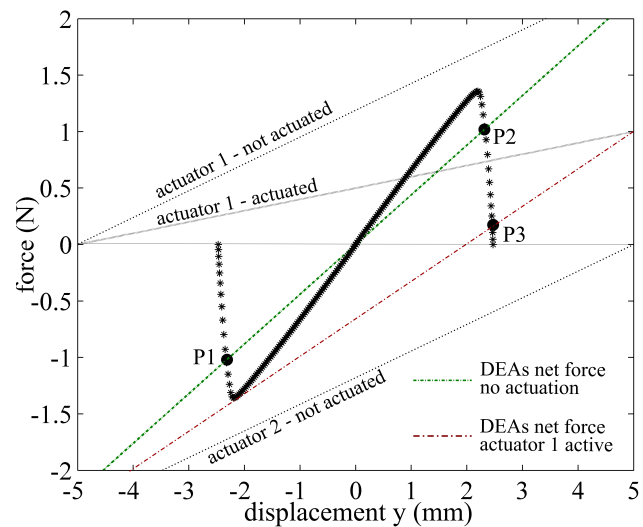


Fig. 9 Results of the FEM simulation. Black dots represent the equilibrium points given by the change in the spring rate of the conical actuator DEA 1. The green dotted line is the sum of the forces of the springs in not-actuated state, the red broken line is the sum of the forces when DEA 1 is activated. The system is first in position P1, then switches to P2 when DEA 1 is active, and in the third phase it stabilizes at P3 when voltage is removed from DEA 1.

References

1. Jasmina Casals-terr , Andreu Fargas-marques, and Andrei M Shkel. Snap-Action Bistable Micromechanisms Actuated by Nonlinear Resonance. *Journal of Microelectromechanical Systems*, 17(5):1082–1093, 2008.
2. M Follador, A T Conn, B Mazzolai, and J Rossiter. Active-elastic bistable minimum energy structures. *Applied Physics Letters*, 105:141903, 2014.
3. Patrick Chouinard and Jean-S bastien Plante. Bistable Antagonistic Dielectric Elastomer Actuators for Binary Robotics and Mechatronics. *IEEE/ASME Transactions on Mechatronics*, 17(5):857–865, October 2012.
4. Seunghoon Park and Dooyoung Hah. Pre-shaped buckled-beam actuators: Theory and experiments. *Sensors and Actuators A: Physical*, 148(1):186–192, November 2008.
5. M. Hafez, M.D. Lichter, and S. Dubowsky. Optimized binary modular reconfigurable robotic devices. *IEEE/ASME*

- Transactions on Mechatronics*, 8(1):18–25, March 2003.
6. W.K. Schomburg and C. Goll. Design optimization of bistable microdiaphragm valves. *Sensors and Actuators A: Physical*, 64(3):259–264, January 1998.
 7. Seung-Won Kim, Je-Sung Koh, Jong-Gu Lee, Junghyun Ryu, Maenghyo Cho, and Kyu-Jin Cho. Flytrap-inspired robot using structurally integrated actuation based on bistability and a developable surface. *Bioinspiration & biomimetics*, 9(3):036004, March 2014.
 8. Tiefeng Li, Zhanan Zou, Guoyong Mao, and Shaoxing Qu. Electromechanical Bistable Behavior of a Novel Dielectric Elastomer Actuator. *Journal of Applied Mechanics*, 81(4):041019, November 2013.
 9. K. Tadakuma, L.M. DeVita, J.S. Plante, Y. Shaoze, and S. Dubowsky. The experimental study of a precision parallel manipulator with binary actuation: With application to MRI cancer treatment. In *Robotics and Automation. ICRA 2008. IEEE International Conference on*, pages 2503–2508, Pasadena, CA, May 2008. IEEE.
 10. Federico Carpi, Danilo De Rossi, Roy Kornbluh, Ronald Edward Pelrine, and Peter Sommer-Larsen. *Dielectric Elastomers as Electromechanical Transducers*. 2011.
 11. a T Conn and J Rossiter. Towards holonomic electroelastomer actuators with six degrees of freedom. *Smart Materials and Structures*, 21(3):035012, March 2012.
 12. J-S Plante and S Dubowsky. On the properties of dielectric elastomer actuators and their design implications. *Smart Materials and Structures*, 16(2):S227–S236, April 2007.
 13. M Hodgins, a York, and S Seelecke. Modeling and experimental validation of a bi-stable out-of-plane DEAP actuator system. *Smart Materials and Structures*, 20(9):094012, September 2011.
 14. M Hodgins, a York, and S Seelecke. Experimental comparison of bias elements for out-of-plane DEAP actuator system. *Smart Materials and Structures*, 22(9):094016, September 2013.
 15. L M Devita, J S Plante, and S Dubowsky. The Design of High Precision Parallel Mechanisms using Binary Actuation and Elastic Averaging : With Application to MRI Cancer Treatment MIT. pages 1–7, 2007.
 16. Mattias Vangbo. An analytical analysis of a compressed bistable buckled beam. *Sensors and Actuators A: Physical*, 69(98):212–216, 1998.
 17. G Berselli, R Vertechy, G Vassura, and V Parenti-Castelli. Optimal synthesis of conically shaped dielectric elastomer linear actuators: Design methodology and experimental validation. *Mechatronics, IEEE/ASME Transactions on*, 16(1):67–79, 2011.